CONTRIBUTION FROM THE BAKER LABORATORY OF CHEMISTRY,
CORNELL UNIVERSITY, ITHACA, NEW YORK 14850

Magnetic, Electron Spin Resonance, Optical, and Structural Studies of the Isomorphous Series Na(Sc,Fe)TiO_4[1]

BY A. F. REID, H. K. PERKINS, AND M. J. SIENKO

Received July 17, 1967

The isomorphous series $NaSc_{1-x}Fe_xTiO_4$ has been studied in powder form. Cell dimensions decrease regularly as x increases, and magnetic susceptibilities follow a Curie–Weiss law $\chi = C(T + \theta)^{-1}$ from $T = 380°K$ to $T = \theta°K$. The Weiss constant θ increases from 15 to 280° as x goes from 0 to 1, and the effective magnetic moment $2.828C^{1/2}$ decreases from a spin-only value of 5.93 BM at $x = 0.01$ to a minimum of 5.62 BM at $x = 0.5$. Optical reflectance spectra show at low Fe^{3+} concentration a strong band at 28,600 cm^{-1} which fades and is replaced by one at 24,000 cm^{-1} at higher concentrations. This change is coincident with replacement of a sharp esr line at $g' = 4.27$ by a broad line centered at $g' = 2$. Observed properties are interpreted in terms of isolated Fe^{3+} ions in rhombic crystal-field sites at low Fe^{3+} concentrations and superexchange-coupled Fe^{3+}–O–Fe^{3+} pairs in distorted octahedral sites at higher Fe^{3+} concentrations.

Introduction

Although calcium ferrite, $CaFe_2O_4$, has the appropriate stoichiometry for a spinel, its structure is not spinel but that corresponding to space group Pnma, No. 62, wherein Fe(I) and Fe(II) occupy crystallographically inequivalent distorted octahedral sites and Ca is nine-coordinate.[2] As part of a continuing program in this laboratory to study electron-transport properties in transition metal oxides, we have synthesized a series of isomorphous compounds of the type $NaScTiO_4$[3] which have $CaFe_2O_4$ structure except that Sc^{3+} and Ti^{4+} randomly substitute for the two Fe^{3+} and, in the role of charge-compensating ion, Na^+ replaces Ca^{2+}. $NaFeTiO_4$, which also has the $CaFe_2O_4$ structure, was observed to form a continuous series of solid solutions with $NaScTiO_4$, so it became of interest to study this system as a possible framework for investigating Fe^{3+}–Fe^{3+} interactions as a function of increasing Fe^{3+} concentration.

Originally, it was believed that $NaScTiO_4$ possessed an empty conduction band, resulting from direct overlap of 3d orbitals or indirect overlap through intervening oxygen atoms, which could be populated electronically by appropriate substitution of a donor-trivalent ion for Sc^{3+}. As it turned out,[3] only Fe^{3+} would substitute for Sc^{3+} and all of the materials prepared were insulators. The conduction band in these materials must therefore be considerably higher than the localized electron levels, and magnetic interactions, if they do occur, need to be explained by conventional exchange couplings.

In addition to the synthetic work involved in preparing the materials, the present paper describes magnetic susceptibility, X-ray, esr, optical absorption, and Mössbauer studies on $NaSc_{1-x}Fe_xTiO_4$ as a function of progressive replacement of Fe^{3+} for Sc^{3+}.

(1) This research was sponsored by the Air Force Office of Scientific Research, Office of Aerospace Research, United States Air Force, under AFOSR Grant No. 796-67 and was supported in part by the Advanced Research Projects Agency through the Materials Science Center at Cornell University.

(2) B. F. Decker and J. S. Kasper, *Acta Cryst.*, **10**, 332 (1957); P. M. Hill, H. S. Peiser, and J. R. Rait, *ibid.*, **9**, 981 (1956).

(3) A. F. Reid, A. D. Wadsley, and M. J. Sienko, *Inorg. Chem.*, **7**, 112 (1968).

Experimental Section

Preparation of Compounds.—$NaScTiO_4$, $NaFeTiO_4$, and $NaScTiO_4$ containing Fe^{3+} substituted for Sc^{3+} were prepared by heating in air in platinum dishes finely ground mixtures of sodium oxalate with appropriate metal oxides first at 600° and then at 950–1000° for 15 hr, followed by regrinding and further heating. Monitoring of product weight confirmed that the oxygen defect, if any, was less than 0.005%. Sodium oxalate was analytical reagent grade; TiO_2 was Fisher Certified reagent. Fe_2O_3 was laboratory reagent grade. Sc_2O_3, 99.5%, was obtained from the Australian Mineral Development Laboratories, South Australia, and contained 0.3% SiO_2 as the chief impurity.

X-Ray Diffraction Data.—Powder diffraction data were obtained with a General Electric XRD-5 diffractometer, using Ni-filtered copper Kα radiation. For Fe compounds, the rate meter input was arbitrarily biased to place the fluorescence background near zero on the chart recording, and diffraction intensities were measured above the background. Chart recordings were at slow scan rates (0.2°/min). The diffractometer 2θ scale was calibrated with W and Si powders, and W powder was included as an internal standard in all samples. After preliminary indexing, an iterative index selection and least-squares refinement program was employed to determine precise lattice parameters. Final parameters were determined from reflections in the 2θ range 60–90°. For each compound examined, the standard deviation in $\sin^2\theta_{calcd} - \sin^2\theta_{obsd}$ was approximately 10×10^{-5}.

Magnetic Susceptibility.—Susceptibilities were determined from 77 to 360°K using a Gouy balance arrangement sensitive to 2×10^{-9} cgs unit. $Hg(NCS)_4$,[4] sieved to a series of mesh sizes, was employed as the standard and measurements were taken at fields from 2500 to 10,000 gauss at each temperature point. Pyrex sample tubes, either 3 or 6 mm in diameter, with a septum at the pole gap center and an evacuated extension 10–11 cm below the septum were used to obviate tube corrections. No change in weight, within 0.00002 g, could be detected when full field was applied to an empty tube at room temperature.

The susceptibility correction for the host lattice (and in fact any necessary correction for buoyancy effects or noncancellation of tube pull at any other temperatures) was obtained by directly measuring the susceptibility of $NaScTiO_4$. At 300°K, the molar susceptibility was found to be -66×10^{-6} cgs unit compared with -64×10^{-6} cgs unit calculated from the atomic diamagnetic susceptibility values listed by Selwood.[5] However, the apparent susceptibility, although independent of field, was not constant with temperature, being -97×10^{-6} at 373°K and $+150 \times 10^{-6}$ at 77°K, indicating either a paramagnetic impurity, and fortui-

(4) H. Schwarz, *Z. Anorg. Allgem. Chem.*, **323**, 44 (1963).

(5) P. W. Selwood, "Magnetochemistry," 2nd ed, Interscience Publishers, Inc., New York, N. Y., 1956.

TABLE I
LATTICE CONSTANTS FOR $NaSc_{1-x}Fe_xTiO_4$, A

	x = 0	0.10	0.25	0.50	0.75	0.875	1.00
$a \pm 0.003$	9.277	9.275	9.255	9.233	9.202	9.184	9.175
$b \pm 0.002$	3.048	3.042	3.030	3.009	2.985	2.969	2.962
$c \pm 0.004$	10.917	10.904	10.879	10.832	10.779	10.747	10.741

tous agreement at 300°K, or some extraneous effect. Corrections based on these values were applied to the gram susceptibilities observed for various concentrations of Fe^{3+} before calculation of paramagnetic gram-atomic susceptibilities.

Electron Spin Resonance.—Esr spectra were examined at 77 and at 300°K, using standard homodyne systems operating at 9.5 GHz (X band) and 35 GHz (Q band) with balanced crystal detection and 100-kHz field modulation.

Optical and Near-Infrared Spectra.—Reflection spectra from 40,000 to 3800 cm^{-1} were obtained by diffuse reflectance using a Beckman DK-2A double-beam recording spectrophotometer fitted with a reflectance sphere and housing. $NaScTiO_4$ was used as a reference sample, to obviate interference by the strong ultraviolet absorption shown by titanate lattices.[6]

Results

Bond Lengths and Angles.—Lattice parameters for the composition $NaSc_{1-x}Fe_xTiO_4$ for x = 0–1 are given in Table I. The change in unit-cell edges was not linear with composition but tended to flatten out at either end of the range, as shown in Figure 1. Planim-

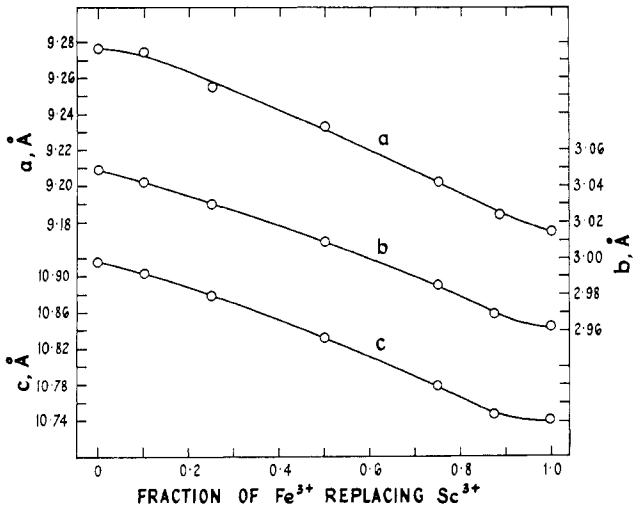

Figure 1.—Lattice parameters a, b, and c as a function of increasing substitution of Fe^{3+} for Sc^{3+} in $NaScTiO_4$.

eter comparison of the diffraction peak areas from 16 to 90° for 2θ at compositions x = 0, 0.10, 0.25, 0.50, and 1.00 revealed no intensity anomalies, and it can be assumed that no changes in ordering and only small changes in fractional atomic coordinates occur. Assuming $NaScTiO_4$ fractional coordinates[3] and using the lattice parameters from Table I, metal–metal and metal–oxygen separations were calculated. Despite the change in the a/b ratio for x = 0–1 these separations were accurately proportional to the b axis length over the range of x. Pertinent separations are shown in Table II for $NaScTiO_4$ and $NaFeTiO_4$.

Figure 2 shows the disposition of metal sites and

(6) A. F. Reid and M. J. Sienko, *Inorg. Chem.* **6**, 321 (1967).

TABLE II
SELECTED[a] BOND ANGLES AND METAL–METAL AND METAL–OXYGEN SEPARATIONS

	$NaScTiO_4$	$NaFeTiO_4$
	Separation, A	
M(1)–M(1) direct[b]	3.048 ± 0.003	2.962 ± 0.003
M(1)–M(1) oblique[b]	3.114 ± 0.006	3.06 ± 0.01
M(2)–M(2) direct	3.048 ± 0.003	2.962 ± 0.003
M(2)–M(2) oblique	3.137 ± 0.006	3.08 ± 0.01
M(1)–M(2) corner-shared	3.615 ± 0.006	3.56 ± 0.01
M(1)–O(1)	2.069 ± 0.015	2.03 ± 0.03
M(1)–O(3)	2.065 ± 0.015	2.03 ± 0.03
M(1)–O(4)	2.052 ± 0.015	2.01 ± 0.03
M(1)–O(4′)	2.004 ± 0.015	1.97 ± 0.03
	Angle, deg	
O(1)–M(1)–O(4)	84.6	85.6
O(1)–M(1)–O(4) diagonal	179.2	179.23
O(1)–M(1)–O(3)	93.4	93.6
O(1)–M(1)–O(4′)	100.9	101.0
O(4)–M(1)–O(4)	95.9	95.0

[a] The metal–oxygen octahedra for metal atoms at crystallographic sites 2 are slightly more regular and show less range in bond length and bond angle than those shown by sites 1. [b] All atoms lie in planes $y = 1/4$ or $y = 3/4$. "Direct" distance is measured parallel to the b axis and is equal to the b-axis length. "Oblique" distance is between equivalent sites in $y = 1/4$ and $y = 3/4$ planes.

oxygens for a section of a double block of sites 1 viewed up the b axis for $NaScTiO_4$ and $NaFeTiO_4$, and Figure 3 shows the bond lengths and angles for a part of the double block. The angles shown between edge-shared oxygens and the metal atoms they connect in the b direction indicate that a small compression of the metal–oxygen octahedra to a slightly more regular disposition occurs as Fe^{3+} replaces Sc^{3+} and the b axis decreases from 3.048 to 2.962 A. The other angles in the octahedra, Table II, show no significant changes. The octahedra for metal atoms at site 2 are slightly more regular than those at site 1 and are not included in Table II.

Magnetic Susceptibility. For x = 0.01–1.00 $NaSc_{1-x}Fe_xTiO_4$ compositions all show field-independent paramagnetism. The Curie–Weiss relationship χ (per g-atom of Fe^{3+}) = $C/(T + \theta)$ was obeyed from 380°K down to approximately the Weiss temperature. Plots of $1/\chi$ *vs.* T are given in Figure 4. Magnetic constants calculated from the linear portions of the plots are given in Table III. Magnetic moments were calculated from the relation $\mu_{eff} = 2.828 \cdot C^{1/2}$. For Fe^{3+} the spin-only magnetic moment value of 5.92 BM is closely approximated for 1% of Fe^{3+} substituted for Sc^{3+}, as expected for magnetically dilute species. While the Weiss constant θ shows a steady increase with Fe^{3+} concentration, the Curie constant C (and the magnetic moment μ_{eff}) decreases

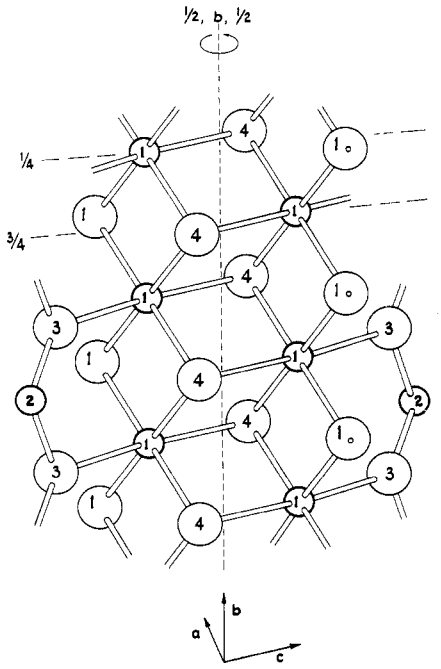

Figure 2.—View of a double group of octahedral sites of kind 1 viewed up the b axis. Small circles are metal atom sites; large circles, oxygen. Numbering corresponds to that in Table II.

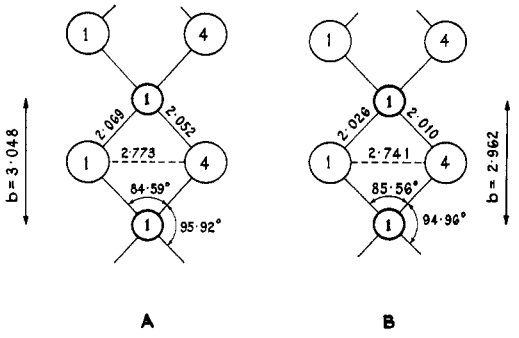

Figure 3.—Metal–oxygen separations about metal site 1 in $NaScTiO_4$ (designated by A) and $NaFeTiO_4$ (designated by B). Small circles are metal atom sites; larger circles, oxygen.

initially and has a minimum at about $x = 0.5$. (See Figure 5.)

Optical Spectra.—Up to $x = 0.05$, as represented by curve A in Figure 6, the diffuse reflection spectrum of $NaSc_{1-x}Fe_xTiO_4$ shows three absorption bands, at 28,600, 20,800, and 9800 cm^{-1}, respectively. As the Fe^{3+} concentration is increased, the intensity of the highest frequency band passes through a maximum at about $x = 0.05$. (See Table IV.) By $x = 0.10$, and possibly at $x = 0.05$, a separate band at 24,400 cm^{-1} is evident; this strong band has replaced the other by $x = 0.25$ and continues to increase in intensity with Fe^{3+} concentration. The two, relatively weaker, lower frequency bands show a continual increase in intensity with concentration from $x = 0$ to $x = 1$. No other absorption bands, at energies down to 3800 cm^{-1}, were observed at any Fe^{3+} concentration. The slope of the high-frequency side of the 28,000 cm^{-1} band is to some extent a function of the cancellation of the host lattice ultraviolet absorption by that of the $NaScTiO_4$ reference sample, but it is not a result of instrument

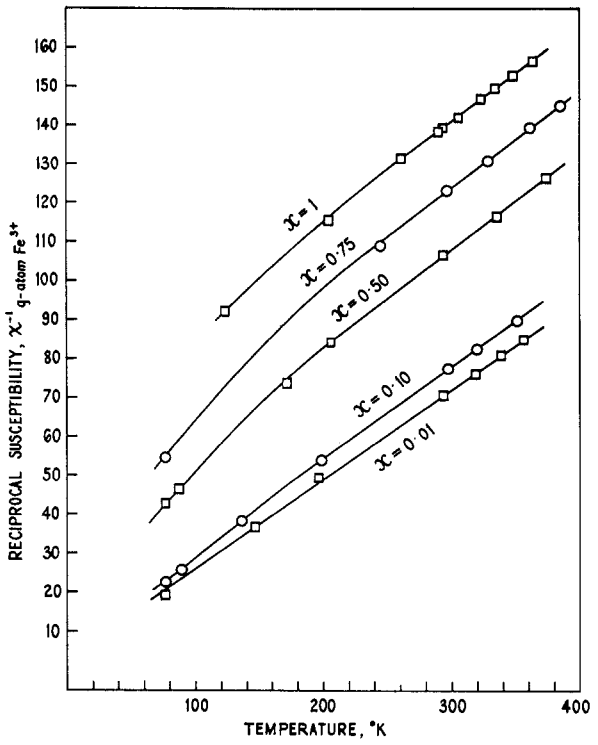

Figure 4.—Reciprocal susceptibility per g-atom of Fe^{3+} (after correction for diamagnetism) as a function of temperature for $NaSc_{1-x}Fe_xTiO_4$ at various values of x.

TABLE III

PARAMAGNETIC CONSTANTS FOR $NaSc_{1-x}Fe_xTiO_4$

χ (per g-atom of Fe^{3+}) $= C/(T + \theta)$ cgs units

x	C	θ	μ_{eff}
0.00	4.42[a]	15.0[a]	5.95[a]
0.01	4.401 ± 0.050	16.5 ± 1.8	5.93
0.10	4.188 ± 0.038	25.4 ± 1.6	5.79
0.50	3.953 ± 0.047	125 ± 1.5	5.62
0.75	4.052 ± 0.083	203 ± 1.5	5.69
1.00	4.112 ± 0.030	270 ± 2	5.73

[a] Extrapolated value.

cutoff. At $x = 0.02$, 0.10, and 0.25 it was found possible to obtain in the ultraviolet region a flat tail at a $-\log (R/R_0)$ value of less than 0.1, extending from 30,000 to above 40,000 cm^{-1} and indicating that lattice absorption was correctly balanced out. In Table IV the values of $-\log (R_{sample}/R_{reference})$ are given in parentheses next to each frequency value. All samples were of similar particle size, −230 to +325 mesh, so the logarithmic reflectance ratios give semiquantitative relative values of the molar extinction coefficients at each concentration.[7] Table IV shows that for the two lower frequency bands, plots of $-\log (R/R)_0$ would indeed be reasonably linear with concentration up to $x = 0.5$. At higher concentrations and intensities, absorption becomes too strong to allow meaningful comparisons.

The 28,600-cm^{-1} band at low Fe^{3+} concentration and the 24,400-cm^{-1} band replacing it above 10% Fe were both found to have frequencies sensitive to concentration (or lattice dimensions). The frequencies of the

(7) W. W. Wendlandt and H. G. Hecht, "Reflectance Spectroscopy," Interscience Publishers, Inc., New York, N. Y., 1966.

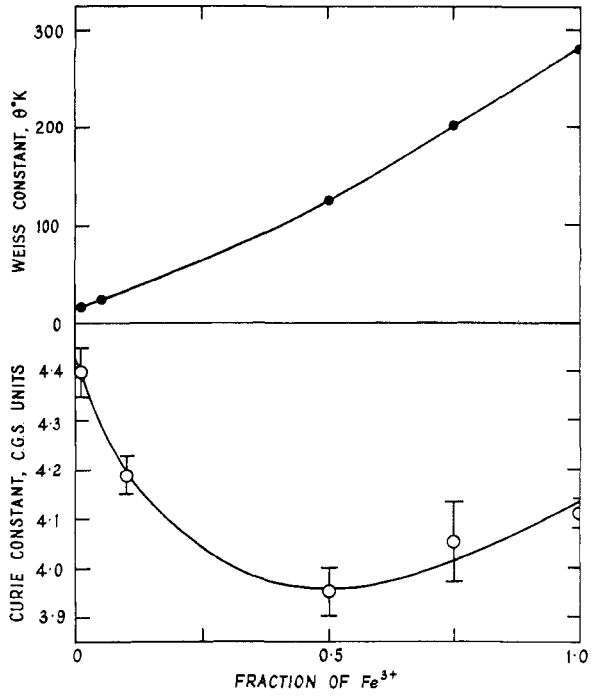

Figure 5.—Curie constant C and Weiss constant θ in $\chi = C/(T + \theta)$ for $NaSc_{1-x}Fe_xTiO_4$ as a function of fraction Fe^{3+} substituted for Sc^{3+}.

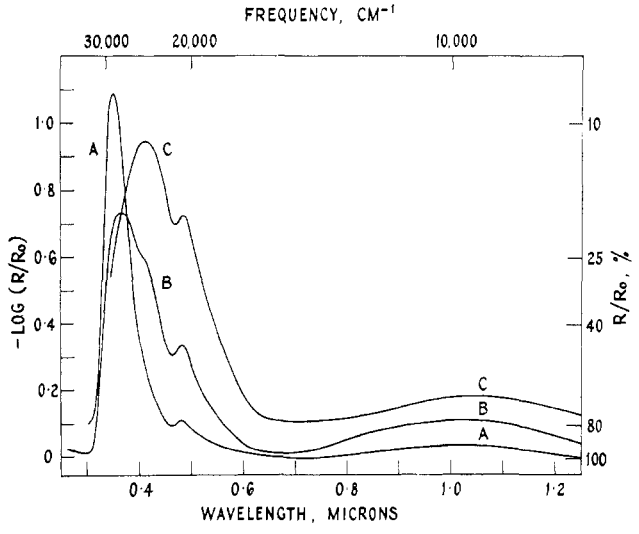

Figure 6.—Reflectance spectra showing absorption by $NaSc_{1-x}Fe_xTiO_4$ as a function of wavelength: curve A, x = 0.02; curve B, x = 0.10; curve C, x = 0.25. R/R_0 is the ratio of the incident light intensities reflected by the sample and the reference sample ($NaScTiO_4$), respectively.

TABLE IV

REFLECTION SPECTRA OF $NaSc_{1-x}Fe_xTiO_4$ at 300°K

$[Fe^{3+}]$,	Freq, cm^{-1}			
%	Band 1	Band 2	Band 3	Band 4
1.0	28,600 (1.1)[a]	...	20,800 (0.05)	9850 (0.01)
2.0	28,400 (1.2)	...	20,700 (0.1)	9800 (0.02)
5.0	27,700 (1.9)	...	20,650 (0.3)	9800 (0.05)
10.0	27,400 (0.7)	24,400 (0.55)	20,750 (0.35)	9680 (0.10)
25	...	24,200 (0.95)	20,650 (0.70)	9660 (0.18)
50	...	23,400 (1.25)	20,750 (1.15)	9520 (0.3)
75	...	22,200 (1.4)	20,400 (1.4)	9420 (0.7)
100	...	22,200 (1.3)	20,400 (1.3)	9260 (0.5)

[a] Numbers in parentheses give relative logarithmic heights of recorded reflection peaks.

other two bands, present throughout, were relatively insensitive to concentration. All bands showed an increase in frequencies in spectra obtained at 80°K. Band 1 showed a shift of about 200–300 cm^{-1}, while band 2 showed an apparently similar shift at 0.10 but a lesser shift at higher Fe^{3+} concentrations—*e.g.*, 100 cm^{-1} at x = 0.25. Band 3, the sharpest, was most easily measured for shifts with temperature. These appeared to be constant from x = 0.05 to x = 0.25 at least, and a shift of 190 ± 30 cm^{-1} was observed at x = 0.25 on cooling the sample from 300 to 80°K, with similar values at lower concentrations. The broadness of the band at 9660 cm^{-1} prevented any shift from being observed at least to x = 0.25. Also, at 80°K, and x = 0.25, a new band at 15,100 cm^{-1} was evident, with $-\log (R/R_0)$ approximately equal to 0.1. This band was much weaker at x = 0.1 and stronger at x = 0.5 and above, but obscured at room temperature in each case.

Electron Spin Resonance.—The esr spectra obtained on powder samples of $NaSc_{1-x}Fe_xTiO_4$ at 9.5 GHz and 300°K are shown in Figures 7 and 8. At the lowest Fe^{3+} concentration (x = 0.01), there was a single, intense, low-field line with a g' value of 4.27. (g' is defined experimentally as $h\nu/\beta H$, where ν is the microwave frequency, H is the magnetic field, h is the Planck constant, and β is the Bohr magneton.) Measurement of the x = 0.01 sample at 35 GHz did not give the intense g' = 4.27 line but only weak, broad, asymmetrical lines around g' = 2 and 4. At 9.5 GHz, as the Fe^{3+} concentration was increased to x = 0.10, the g' = 4.27 line persisted but was accompanied by a 1600-gauss-wide line centered at g' = 2.00 and a 60-gauss-wide line centered at g' = 1.95. The line widths of the 4.27 and 2.00 lines did not change in going from room to liquid nitrogen temperature, but the ratio of their peak-to-peak heights increased by a factor of 2.3. With Fe^{3+} concentrations at $x \geq 0.25$, the g' = 4.27 line has disappeared. There was only the very broad line at g' = 2, except for x = 1 where the line was considerably narrowed and changed in shape.

Mössbauer Spectra.—Mössbauer results were obtained at room temperature. For x = 0.01 in $NaSc_{1-x}Fe_xTiO_4$, the observed isomer shift relative to natural iron was approximately 0.2 mm/sec, with a poorly resolved quadrupole splitting of 0.28 mm/sec. With x = 0.10, 0.25, and 1.00, much better spectra were obtained. Isomer shifts and quadrupole splittings were 0.38, 0.41, and 0.41 mm/sec and 0.64, 0.60, and 0.46 mm/sec, respectively. The isomer shifts are appropriate to Fe^{3+}, not Fe^{2+}, and the quadrupole splittings indicate that the Fe^{3+} is in asymmetrical sites. The decrease in the quadrupole splitting observed for x = 1 is beyond experimental error.

Discussion

The most striking aspect of this work is that whereas there is only a small, rather gradual change in structural parameters as Fe^{3+} substitutes for Sc^{3+}, there is a

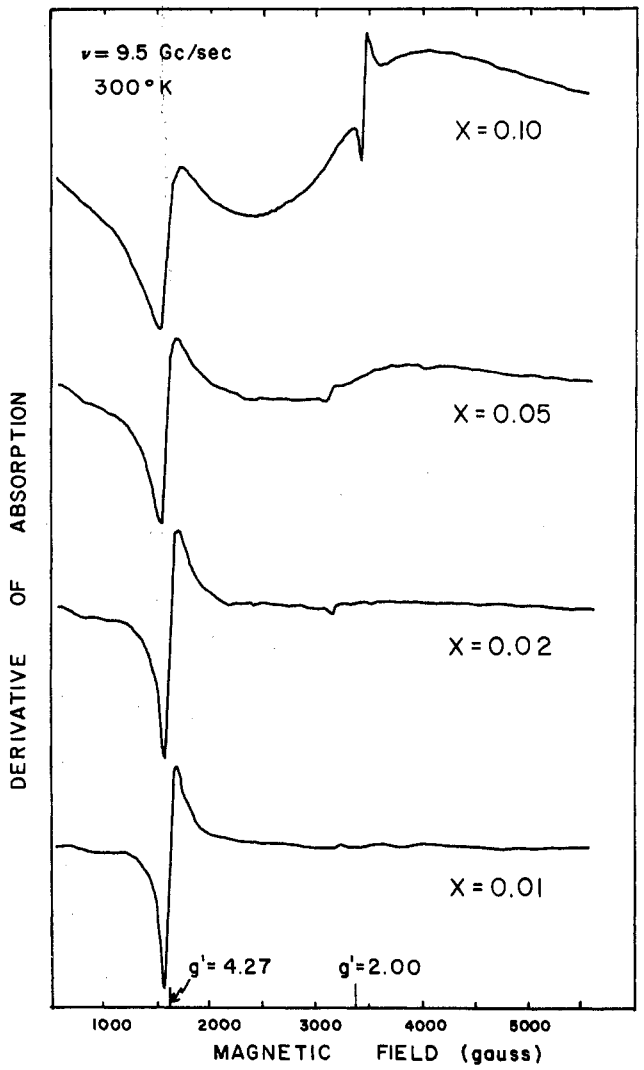

Figure 7.—Esr spectra of $NaSc_{1-x}Fe_xTiO_4$ powders at low Fe^{3+} concentrations. Microwave frequency was 9.5 GHz; temperature, 300°K. The line at $g' = 4.27$ (where $g' = h\nu/\beta H$) is attributed to Fe^{3+} ($3d^5$) in a rhombic crystal-field environment; the line at $g' = 2.00$, to exchange-coupled Fe^{3+} ions.

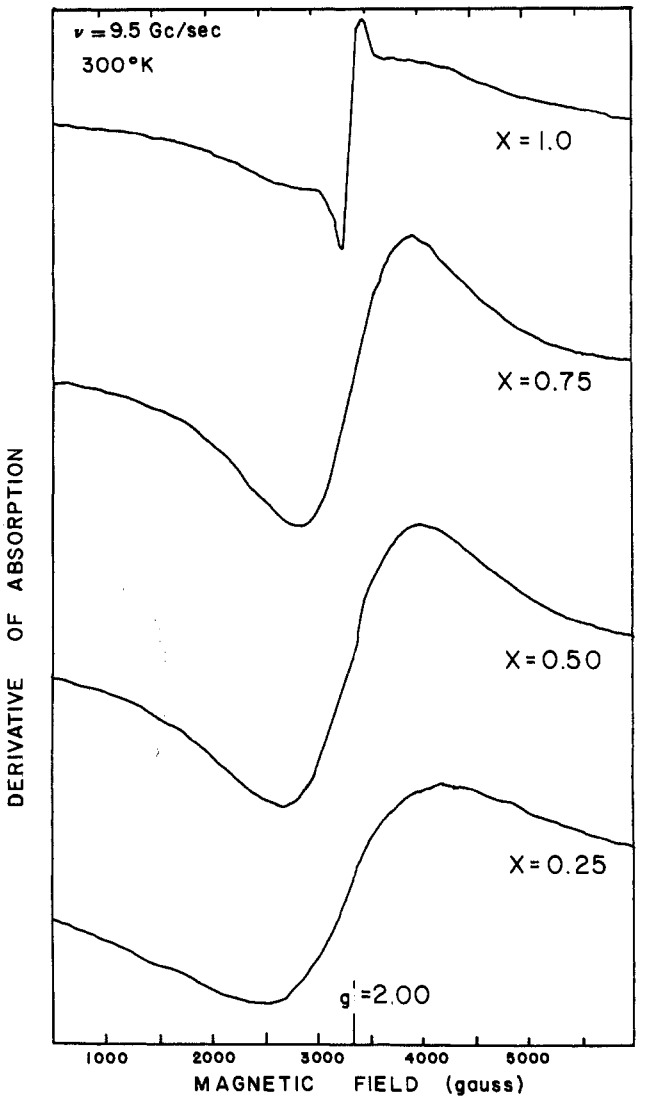

Figure 8.—Esr spectra of $NaSc_{1-x}Fe_xTiO_4$ at high Fe^{3+} concentrations. Microwave frequency was 9.5 Gc/sec; temperature, 300°K.

pronounced change in the character of the species giving rise to the optical and magnetic resonance absorptions. That the rhombic a, b, and c parameters should change only slightly is not surprising. The radii of Sc^{3+} and Fe^{3+} are 0.81 and 0.64 A, respectively, according to Ahrens,[8] and even closer, 0.69 and 0.63, respectively, according to the perovskite-fitted values of Geller.[9] The detailed structures of $NaScTiO_4$ and $NaFeTiO_4$ are discussed elsewhere,[3] but the salient feature is that the M^{3+} ions (Sc^{3+} or Fe^{3+}) and the M^{4+} ions (Ti^{4+}) substitute randomly for the two kinds of Fe in the $CaFe_2O_4$ structure and are indeed constrained by the structure to adopt equivalent bond lengths. There are eight transition metal atoms per unit cell, contained in four sets of pairs of slightly distorted, edge-shared oxygen octahedra. The pairs, or double blocks, of oxygen octahedra are joined to other double blocks by corner sharing. The metal atom sites in each double block are crystallographically equivalent and repeat infinitely in the b direction in crystallographically equivalent sets generated by the twofold screw axis of the Pnma space group as shown in Figure 2. Each double block (or string of double blocks) is corner-connected to a double block containing metal atom sites of the crystallographically alternate kind, the two kinds being referred to as M(1) and M(2) in Table II. The internal symmetries of the two nonequivalent sets of double blocks are very similar, and bond distances are almost the same for the two sets. The X-ray studies do not exclude the possibility that ordering in the b direction of M^{3+} and M^{4+} occupancy occurs within any given string of double blocks unrelated to that in the adjacent corner-connected blocks.

The random occupancy of Sc^{3+} and Ti^{4+} in the M(1) and M(2) sites makes it difficult to predict the precise environment of Fe^{3+} as substitution of Fe^{3+} for Sc^{3+} progresses. On a statistical basis, the chance that Fe^{3+} ions at low concentration occur in adjacent octahedra is quite small, so the low-concentration absorption peak and esr line must be attributed to "iso-

(8) L. H. Ahrens, *Geochim. Cosmochim. Acta*, **2**, 155 (1952).
(9) S. Geller, *Acta Cryst.*, **10**, 249 (1957).

lated" Fe^{3+} ions. M(1)–M(1) and M(2)–M(2) separations are greater than the critical 2.93-A Fe^{3+}–Fe^{3+} spacing predicted by Goodenough[10] for direct d-orbital overlap, and the fact that the observed magnetic moment of Fe^{3+} is close to spin-free $3d^5$ indicates that the number of directly coupled Fe^{3+}–Fe^{3+} pairs must be small.

A more likely kind of coupling between Fe^{3+} ions, which would appear at higher concentrations of Fe^{3+}, would be superexchange coupling through oxygen atoms. Given random positioning of M^{3+}–M^{4+} in one double block with respect to the M^{3+}–M^{4+} pair in an adjacent double block down the *b*-axis chain, the number of Fe^{3+}–O–Fe^{3+} interactions should increase in proportion to the mole fraction of Fe^{3+} substituted for Sc^{3+}. Even if there were M^{3+} ordering along the *b*-axis chain, the number of Fe^{3+}–O–Fe^{3+} interactions would show the same proportionality. The fact that the Weiss temperature of Figure 5 is almost exactly proportional to the mole fraction of Fe^{3+} supports the conclusion that there is antiferromagnetic coupling between the Fe^{3+} ions. Such coupling is expected to be particularly strong between high-spin d^5 ions, since correlation effects on the intervening $p\sigma$ oxygen assure oppositely directed moments on the two ions joined by superexchange. The situation is similar to that found in ZnF_2-diluted MnF_2, where an observed linear dependence of Weiss constant on increasing mole fraction of Mn^{2+} was explained by a simple averaging over the increasing number of exchange interactions between nearest cation neighbors.[11] An interesting second-order feature of the curve in Figure 5 is that the linear dependence of θ on x does not extrapolate to $\theta = 0$ for $x = 0$, as might be expected if the Weiss constant owed its origin exclusively to exchange interaction. The finite θ at infinite dilution of Fe^{3+} suggests there might be an appreciable crystal-field component in θ. Interpretation of θ, however, requires great caution. As noted by Sato, Arrott, and Kikuchi,[12] a linear relation between θ and concentration is to be expected at low concentration only for a Curie–Weiss molecular field model. Other models such as the cluster-variation model, which allow for "magnetically isolated" ions, have θ going to zero long before infinite dilution. The effect of "magnetically isolated" ions may also be the explanation why no Néel temperature was observed for any of our materials. Except when θ is very large, it is rare that Néel temperatures are less than half of θ. Although our measurements were confined to >77°K, it was anticipated that Néel transitions would be observed. (An additional complication exists in this structure in that the M–O–M angles are more favorable to superexchange—*i.e.*, closer to 180 than to 90°—in one set of planes than in the direction perpendicular to those planes. The result is to favor antiferromagnetic coupling in the parallel sections but only weak interactions between sections.)

So far as esr is concerned, at low concentrations of Fe^{3+} in $NaSc_{1-x}Fe_xTiO_4$ the dominant species appear to be isolated Fe^{3+} ions in rhombic crystal-field environments. The single intense esr line at $g' = 4.27$ (Figure 7) corresponds to the $g' = 4.3$ line observed by Castner, Newell, Holton, and Slichter[13] for Fe^{3+} in glass. It can be accounted for by a spin Hamiltonian of the form

$$\mathcal{H} = E(S_x^2 - S_y^2) + g\beta\mathbf{H}\cdot\mathbf{S}$$

where the $E(S_x^2 - S_y^2)$ term, which represents the interactions with a rhombic crystal field, is appreciably larger than the Zeeman term $g\beta\mathbf{H}\cdot\mathbf{S}$. (Wickman, *et al.*,[14] treat the more general crystal-field Hamiltonian, $D[S_z^2 - (1/3)S(S+1)] + E(S_x^2 - S_y^2)$, and show that the case $D = 0$ of Castner, *et al.*, differs only by a transformation of coordinates from their case $D = 3E$.) In zero magnetic field, the $^6S_0$ (d^5) free-ion ground state is split into three equally spaced Kramers doublets with energy separations of $2\sqrt{7}E$. Treating the magnetic field as a perturbation with $g = 2.00$ characteristic of an S state, we find that the middle doublet gives an isotropic g' value of 4.28 while the other two doublets give anisotropic g' values that would be difficult to observe in powdered samples.

The fact that the $x = 0.01$ sample observed at 35 GHz no longer gave an intense $g' = 4.27$ line but only weak asymmetrical lines at $g' = 2$ and 4 suggests that at 35 GHz the Zeeman term can no longer be considered as a perturbation on the crystal-field term. It allows the following crude limits to be placed on the zero-field separations: $0.31\ cm^{-1} < 2\sqrt{7}E \cong 1.2\ cm^{-1}$. From changes in line intensities at liquid helium temperatures, Castner, *et al.*,[13] and Wickman, *et al.*,[14] estimated the separations in their systems to be $0.6\ cm^{-1} < 2\sqrt{7}E < 1.8\ cm^{-1}$ and $2\sqrt{7}E \cong 3\ cm^{-1}$, respectively.

At $x = 0.10$, the Fe^{3+} concentration has become sufficient that Fe^{3+}–O–Fe^{3+} superexchange interactions become significant. For a pair of spins, $\mathbf{S}_1$ and $\mathbf{S}_2$, the interaction can be represented by the exchange Hamiltonian

$$\mathcal{H}_{ex} = -2J\mathbf{S}_1\cdot\mathbf{S}_2$$

which splits the two ^6S free-ion states as shown in Figure 9 for the antiferromagnetic case. The exchange integral J can be related to the order–disorder transition temperature T_N by

$$J = \frac{-3kT_N}{2zS(S+1)}$$

where z is the number of nearest neighbor magnetic ions. Frequently, the θ measured in the Curie–Weiss law is higher than T_N; however, an estimate of J as equal to $-8.4\ cm^{-1}$ can be obtained by using $T_N \cong \theta = 280°$, $Z = 4$, and $S = 5/2$, appropriate for NaFe-

(10) J. B. Goodenough, "Magnetism and the Chemical Bond," Interscience Publishers, Inc., New York, N. Y., 1963, p 266.

(11) L. Corliss, Y. Delabarre, and N. Elliot, *J. Chem. Phys.*, **18**, 1256 (1950).

(12) H. Sato, A. Arrott, and R. Kikuchi, *J. Phys. Chem. Solids*, **10**, 19 (1959).

(13) T. Castner, Jr., G. S. Newell, W. C. Holton, and C. P. Slichter, *J. Chem. Phys.*, **32**, 688 (1960).

(14) H. H. Wickman, M. P. Klein, and D. A. Shirley, *ibid.*, **42**, 2113 (1965).

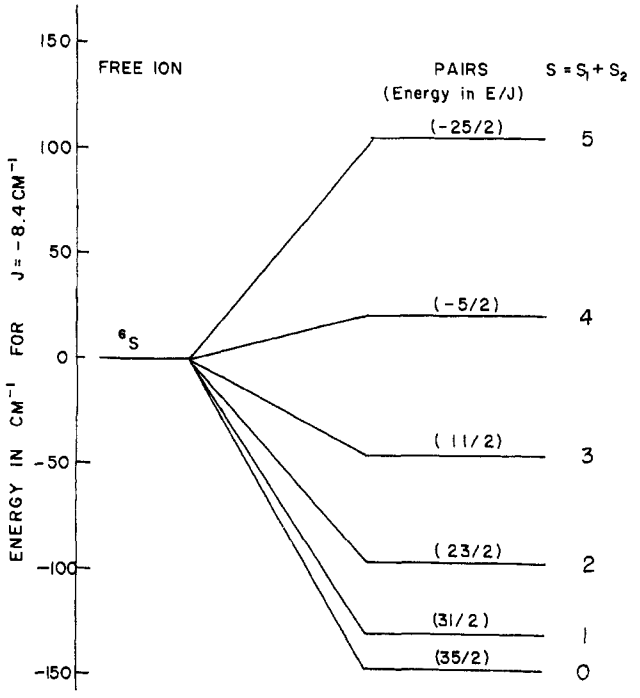

Figure 9.—Energy-level splitting of ^6S ground state due to exchange interaction between a pair of Fe^{3+} ions.

TiO_4. Reference to Figure 9 shows that the smallest energy separations are now 17 cm^{-1}, which should be compared with 0.3-cm^{-1} X-band frequencies, 1-cm^{-1} zero-field single-ion separations, and 210-cm^{-1} thermal energy at 300°K. The isolated ion pairs, consequently, produce spin states $S = 0$–5 that are all occupied at room temperature, spin states that will be split by the crystal field and by the magnetic field.

The nature and magnitude of the crystal field acting on the ion pairs is unknown, but the effect of the Zeeman term in zero crystal field was considered. In this case each of the levels except $S = 0$ should give esr signals with $g' = 2.00$. Bleaney and Stevens[15] show that, assuming line shapes are the same, the intensity of the $M \leftrightarrow M - 1$ transition is proportional to $N[S \cdot (S + 1) - M(M - 1)]/T(2S + 1)$ where N is the number of paramagnetic entities of spin S and M is the electronic magnetic quantum number. In the case of ion pairs, the number N with spin S will depend on the temperature and was calculated using Boltzmann statistics at 300 and 77°K. For all of the states of the ion pairs, the ratio of intensities at 77–300°K was calculated to be 1.7. In the case of isolated Fe^{3+} ions, N is not a function of temperature; the ratio of intensities at 77–300°K is 3.9. As a result, in going from 300 to 77°K the low-field $g' = 4.27$ line associated with isolated ions should increase relative to the $g' = 2.0$ ion-pair line by $3.9/1.7 = 2.3$, which agrees exactly with experiment. The exact agreement is fortuitous in the light of the many approximations made, but the general agreement adds support to the assignment of the broad $g' = 2.0$ line to exchange-coupled ions. The narrow $g' = 1.95$ line visible in Figure 7 for $x = 0.10$ disappeared when the temperature was decreased from 300 to 77°K; this could be explained by assigning it to transitions involving the $S = 5$ or $S = 4$ states. All of the S states are undoubtedly split by the crystal-field term of the Hamiltonian, which was neglected in the above treatment. Such splitting along with magnetic dipolar broadening probably contributes to the broadness of the $g' = 2.0$ line. Mulay and Hofmann[16] report a $g' = 4$ line for mononuclear Fe^{3+}–phenanthroline complexes and a $g' = 2$ line for the binuclear complex having temperature dependences similar to that observed here in the $x = 0.1$ case. At higher concentrations of Fe^{3+}, where the esr spectra of Figure 8 show no $g' = 4.3$ line, a broad $g' = 2.0$ line that narrows with increasing concentration, and a sharp peak on top of the $g' = 2.0$ line at $x = 1$, the isolated pair approach used above is probably no longer valid.

The optical absorption observations are in general agreement with the above model of isolated Fe^{3+} ions and exchange-coupled pairs. Assignment of the absorption bands is, however, difficult because there is a scarcity of data on dilute Fe^{3+} systems to compare with and because much of the interesting information is obscured by what have been labeled[17] charge-transfer band edges at about 20,000 cm^{-1}. We have found, in other studies, that the spectra of octahedrally coordinated Fe^{3+} in $Na_2Fe_2Ti_6O_{16}$ with $Na_2Sc_2Ti_6O_{16}$ as reference[6] and in the Sc_2TiO_5 or $MgTi_2O_5$ lattices (both isomorphous with pseudobrookite, Fe_2TiO_5) with Mg-stabilized Sc_2TiO_5 or $MgTi_2O_5$ as references[18] are quite similar in their general features to the present spectra and have their strongest bands, relatively sharp and intense, at about 25,000–28,000 cm^{-1} with no absorption above 28,000 to at least 40,000 cm^{-1}. In all of these cases the host lattices showed strong ultraviolet absorption, with $-\log (R/R_0) \backsimeq 1$, and an absorption edge at about 25,000 cm^{-1}. Unless a reference sample is used, the Fe^{3+} spectra in these lattices appear to be obscured by strong absorption above about 25,000 cm^{-1}. There appears to be no doubt that the spectra shown in Table IV and Figure 5 are those intrinsic to Fe^{3+} ions or ion pairs and are crystal field bands.

On the basis of the concentration dependence of the four bands shown in Table IV, band 1 can be assigned to isolated Fe^{3+}, band 2 to exchange-coupled pairs, and bands 3 and 4 to both isolated Fe^{3+} and exchange-coupled pairs. For the free Fe^{3+} ion, the ground term is ^6S; excited terms are quadruplets, and, therefore, transitions to them are spin-forbidden. The first excited state is ^4G, which is 32,000 cm^{-1} above the ground term.[19] Assuming as first approximation that the crystal field is octahedral, the ^6S state is unsplit and goes over to $^6A_1$, whereas the ^4G is split into a lowest $^4T_1$, a middle $^4T_2$, and an uppermost ^4E, $^4A_1$.[20] The $^4T_1$ and $^4T_2$ states drop sharply in energy as Dq is increased, but the ^4E, $^4A_1$ states are virtually unchanged.

(15) B. Bleaney and K. W. H. Stevens, *Rept. Progr. Phys.*, **16**, 120 (1953).

(16) L. N. Mulay and N. L. Hofmann, *Inorg. Nucl. Chem. Letters*, **2**, 189 (1966).

(17) K. A. Wickersheim and R. A. Lefever, *J. Chem. Phys.*, **36**, 844 (1962).

(18) W. G. Mumme and A. F. Reid, in process.

(19) U. S. National Bureau of Standards Circular 467, Vol. II, U. S. Government Printing Office, Washington, D. C., 1952, p 65.

(20) Y. Tanabe and S. Sugano, *J. Phys. Soc. Japan*, **9**, 764 (1954).

It is very probable that band 4 observed at 9850 cm^{-1} is due to the $^6A_1 \leftrightarrow {}^4T_1$ (^4G) transition, its great breadth being due to the rapid dropoff with Dq and to the deviation from octahedral symmetry. It is tempting to assign band 3 at 20,800 cm^{-1} to the $^6A_1 \leftrightarrow {}^4T_2$ (^4G) transition, but there are strong arguments against this. For one thing, band 3 is narrow, which would not be expected if it were a transition to a $^4T_2$ state having an important dependence of energy on Dq; secondly, its frequency is practically unchanged as the concentration of Fe^{3+} is increased. Given the lattice shrinkage that accompanies increasing substitution of Fe^{3+} for Sc^{3+} and a probable concomitant increase in Dq, we would expect a significant shift to lower frequency for a $^6A_1 \leftrightarrow {}^4T_2$ transition. It must be that the $^6A_1 \leftrightarrow {}^4T_2$ (^4G) transition is actually hidden between bands 3 and 4, and indeed at 80°K an additional band at 15,100 cm^{-1} was evident in this position. Band 3 can thus be given the more probable assignment $^6A_1 \leftrightarrow {}^4E$, $^4A_1$ (^4G).

Quantitative prediction of expected band positions for Fe^{3+} can be made from the energy matrices of Tanabe and Sugano.[20] However, there is considerable uncertainty as to values appropriate for $10Dq$, B, and C and how to allow for covalence. For $10Dq$, we have selected a value of 13,300 cm^{-1} by interpolating tabulated values[21] for F^- and H_2O on the basis that, of the ligands tabulated, F^- and H_2O are closest to the oxide ligands in our compounds. For B, we have chosen 900 cm^{-1}. This was calculated from $B_0(1 - hk)$, where B_0 is the estimated free-ion value of 1160 cm^{-1}, obtained by adding an observed $d^6 \rightarrow d^5$ increment in Mn^+ to the Fe^{2+} value. Parameter h for ligand oxygen was taken as 0.9 (interpolated between F^- and H_2O); parameter k for Fe^{3+} was tabulated[21] as 0.24. The ratio of the Racah repulsion parameters C/B was taken as 4.0 for Fe^{3+} (extrapolation of the Fe^0, Fe^+, Fe^{2+} values). As suggested by McClure,[22] covalence was most easily allowed for by treating the ^6S–^4G separation in the free ion as an additional parameter. Assuming that band 3 corresponds to the $^6A_1$ (^6S) $\leftrightarrow {}^4A_1$ (^4G), ^4E (^4G) transition, it was necessary to raise the $^6A_1$ level by 6300 cm^{-1}. With this same shift applied to all of the other transitions, the calculated bands for Fe^{3+} in octahedral symmetry are as shown in Table V. The predicted breadth of the bands is based on the slope $dE/d(Dq)$.

Though the agreement shown in Table V is satisfying, it is deceptively so since concentration and temperature dependences of band positions and relative intensities are not fully accounted for. In general, exchange coupling would be expected to broaden the bands (giving an apparent decrease in intensity) and also shift them to lower frequency. However, a shift to higher frequency would occur if the ^6S–^4G separation correction were increased. Further speculation is not warranted, however, on the basis of our data, since they were obtained on powders by diffuse reflectance. The results, nevertheless, are suggestive, and the fundamental importance of magnetic ion interactions is great enough to justify further intensive study of this sytem, particularly in the direction of single-crystal work over a range of temperature as well as over a range of iron concentration.

TABLE V

BAND POSITIONS (cm^{-1}) CALCULATED[a] FOR Fe^{3+}

	Calcd	Obsd (x = 0.10)
$^6A_1$ (^6S) → $^4T_1$ (^4G)	10,100 (wide)	9,680 (band 4)
→ $^4T_2$ (^4G)	15,500 (wide)	(15,100 at 80°K)
→ $^4A_1$ (^4G), ^4E (^4G)	20,700 (narrow)	20,750 (band 3)
→ $^4T_2$ (^4D)	24,200 (narrow)	24,400 (band 2)
→ ^4E (^4D)	27,000 (narrow)	27,400 (band 1)
→ $^4T_1$ (^4P)	32,900 (wide)	...
→ $^4A_2$ (^4F)	38,700 (narrow)	...

[a] $10Dq$ = 13,300 cm^{-1}. B = 900 cm^{-1}. C/B = 4.0.

There remains the possibility that in the region of very low iron concentration (*e.g.*, x = 0.01), the Fe^{3+} is not substitutional for Sc^{3+} but goes elsewhere in the structure. This is considered most unlikely since the structure is rather a dense one and the 3+ and 4+ metals generally go into well-organized positions. The x = 0.01 Mössbauer results, because of their approximate nature, are inconclusive. At face value the isomer shift and the quadrupole splitting suggest that Fe^{3+} in x = 0.01 is different from x = 0.10. At $x \geqq 0.10$, the isomer shifts and quadrupole splittings are appropriate for Fe^{3+} in somewhat asymmetric octahedral environment. At x = 1.00 the quadrupole splitting is significantly less than for x = 0.10 and 0.25. This may be due to the fact that the distortion in the octahedral environment decreases as Sc^{3+} is replaced by Fe^{3+}. In $NaFeTiO_4$, total substitution of Fe^{3+} for Sc^{3+} has placed the Fe^{3+}–O–Fe^{3+} interactions at maximum symmetry and hence reduced the electric field gradient to a minimum. Fe^{2+} is ruled out both by the Mössbauer results and by the absence of oxygen defect, conductivity, and dark color.

Acknowledgment.—We wish to express our appreciation to Dr. Y. Hazony of Princeton University for Mössbauer measurements.

(21) B. N. Figgis, "Introduction to Ligand Fields," Interscience Publishers, Inc., New York, N. Y., 1966, pp 52, 244.

(22) D. S. McClure, *Solid State Phys.*, **9**, 499 (1959).